Influence of anatase and rutile phase in TiO_2 upon the photocatalytic degradation of methylene blue under solar irradiation in presence of activated carbon

J. Matos, R. Montaña, E. Rivero, A. Escudero and D. Uzcategui

ABSTRACT

The influence of activated carbon (AC) on the photocatalytic activity of different crystalline TiO_2 phases was verified in the photocatalytic degradation of methylene blue under UV and solar irradiation. The results showed a volcano trend with a maximum photoactivity for the crystalline phase ratio of anatase:rutile equal to 80:20 both under UV or solar irradiation. By contrast, in presence of AC the photocatalytic activity of the binary materials of TiO_2/AC followed an exponential trend, increasing as a function of the increase in anatase proportion in the TiO_2 framework. The increase in the photoactivity of the binary material TiO_2/AC relative to neat TiO_2 was up to 22 and about 17 times higher under UV and visible irradiation, respectively. The present results suggest that AC interacts more efficiently with anatase phase than with rutile phase.

Key words | activated carbon, anatase, methylene blue, photocatalysis, rutile, TiO_2

J. Matos (corresponding author)
R. Montaña
E. Rivero
A. Escudero
D. Uzcategui
Department of Photocatalysis and Alternative Energies,
Venezuelan Institute for Scientific Research (IVIC),
20632, Caracas 1020-A,
Venezuela
E-mail: *jmatos@ivic.gob.ve*

INTRODUCTION

Nowadays one of the most important challenges for science concern is the study and development of novel advanced oxidation processes (AOPs) for the remediation of polluted water (Andreozzi *et al.* 1999). Among the different AOPs an interesting alternative in the treatment of polluted effluents with dyes such as methylene blue (MB) is the heterogeneous photocatalysis (Houas *et al.* 2007). This technique using titanium dioxide (TiO_2) as photocatalyst has popularity in environmental treatment and purification purposes, but it has some operational limitations such as low adsorption capabilities and only UV absorption of the solar spectra. Between different alternatives to possibly increase the photocatalytic efficiency of TiO_2, one way consists of adding an inert co-adsorbent such as activated carbon (AC) (Torimoto *et al.* 1997). Our group has reported a synergistic effect between both solids in the photomineralization of phenol (Matos *et al.* 1998, 2007), chlorophenols (Matos *et al.* 2001; Cordero *et al.* 2007) and herbicides such as 2,4-D (Matos *et al.* 2001), and has described a scale-up application at real operation conditions at the solar platform at Almería (Herrmann *et al.* 1999). Several other groups have also showed beneficial cooperative effects between TiO_2 and different carbon materials (Araña *et al.* 2003; Tryba *et al.* 2006; Ren *et al.* 2007; Wang *et al.* 2007). A common point of view in these works suggests that the interaction between the semiconductor and carbon material is strongly influenced by the crystalline phase of TiO_2. It is well known (Bakardjieva *et al.* 2006) that titanium dioxide is a semiconductor which crystallizes in three polymorphic forms: rutile, anatase and brookite. It is also well documented that the anatase has the highest photoactivity compared to the brookite or rutile polymorphs (Yanagisawa & Ovenstone 1999). However, the most commercially active photocatalyst (Evonik, ex-Degussa P25) is a three-phase mixture (Bakardjieva *et al.* 2006) of the amorphous, anatase and rutile forms arranged in a complex microstructure, the anatase phase being the greatest fraction with approximately 80% of volume (Hotsenpiller *et al.* 1998). In this sense, many researchers (Bacsa & Kiwi 1998; Ha *et al.* 2000; Bakardjieva *et al.* 2006) have attempted to prepare efficient photocatalysts similar to P25 and understand the metastable thermodynamically mixture of phases. However, few studies have been aimed at verifying the influence of AC on the photocatalytic activity of different crystalline TiO_2 structures. To our knowledge, the present work is the first report on the influence of AC on the photocatalytic activity of different polymorphic crystalline phases of TiO_2. The photocatalytic degradation of MB was chosen as test

doi: 10.2166/wst.2014.127

molecule and both UV and artificial solar irradiation were employed to verify the influence of the irradiation source.

EXPERIMENTAL

Materials

Four as-received commercial TiO_2 products with different crystalline anatasase:rutile ratio were employed as photocatalysts. They were purchased from Riedel & Haen (TiO_2-A_{100}), Merck (TiO_2-A_{95}), Evonik P-25 (TiO_2-A_{80}), and TitaFrance (TiO_2-A_0). A_i denotes the anatasase proportion; i.e. A_{100}, A_{95}, A_{80} and A_0 correspond to 100% (pristine anatasase), 95%, 80%, and 0% (pristine rutile), respectively. One as-received commercial AC from Merck (high purity, <1% ash) was employed. Binary photocatalysts (TiO_2/AC) were obtained by a similar method reported elsewhere (Matos *et al.* 2010a). The binary photocatalysts TiO_2-A_{100}/AC, TiO_2-A_{95}/AC, TiO_2-A_{80}/AC, and TiO_2-A_0/AC were prepared with the relative amount of semiconductor to AC, expressed in mass, i.e. 10:1, by mixing about 63 mg TiO_2 with 6.3 mg AC in 125 mL of deionized H_2O and this slurry was vigorously stirred for 1 h at room temperature. After this, the mixture was filtered and dried for 2 h at 100 °C.

Characterization

Textural characterization was performed by adsorption–desorption N_2 isotherms at 77 K in a Micromeritics ASAP-2020 instrument. The full isotherms in the range of 4×10^{-3} to 84 kPa were perfomed and the BET (Brunauer–Emmett–Teller) method was used to obtain the surface area. Surface pH (pH_{PZC} (point of zero charge)) of bare AC, TiO_2 and a mixture of solids was obtained by the drift method (Lopez-Ramon *et al.* 1999; Cordero *et al.* 2007) by comparing the pH measured after 48 h stirring (to achieve the equilibrium of charges) with that of initial buffer solutions. X-ray diffractometry (XRD) patterns were recorded at room temperature in the 2θ range from 5° to 90° with the Difrac-Plus program on a D-5005 diffractometer from Siemens using the Cu Kα (1.54056) radiation. XRD patterns were processed by Eva program. Fourier transform infra-red experiments were made on a spectrophotometer Magna-IR 560 from Nicolet. The powders were mixed with KBr in a 5% (w/w) mixture and pressed to tablets of 1 cm diameter at 10 tons for 1 min. The spectra were recorded from 4,000 to 400 cm^{-1} with a resolution on 5 cm^{-1}. KBr reference spectrum and CO_2 from ambient were subtracted from every spectrum.

MB photodegradation

The experimental set-up under UV irradiation consists of an open-to-air batch photoreactor (Matos *et al.* 2011). It consists of a 200 mL cylindrical flask made of Pyrex with a bottom optical window of 6 cm in diameter. Irradiation was provided using a 250 W Hg lamp (L_{Hg}) UV. Irradiation was filtered by a circulating water cell (thickness *ca.* 2.0 cm) to remove IR beams and prevent any heating of the suspension. Additional experiments were performed under artificial solar irradiation by using a solar simulator box (XPS-1000-Xe) with a 400 W high pressure Xe lamp. Radiation flux was verified by using a pyranometer (Solar Light PMA2100) and total photon fluxes were estimated as about 1.23×10^{17} and 1.97×10^{17} photons cm^{-2} s^{-1} for Hg lamp (Matos *et al.* 2011) and Xe lamps, respectively. Hg lamp showed about 100% UV spectra while Xe lamp emits a similar solar spectra (Matos *et al.* 2010a) with only about 6% UV. The photocatalytic tests were performed at 25 °C under stirring using 62.5 mg of photocatalysts and 6.3 mg AC in 125 mL MB (12.5 ppm (39.1 μmol/L) initial concentration). The samples were maintained in the dark for 60 min in order to complete adsorption at equilibrium and then the suspension was irradiated. After centrifugation MB aliquots were analyzed using an UV spectrophotometer (PerkinElmer Lambda 35) at 664 nm, and the MB concentrations were estimated using a standard calibration curve. Photoactivity tests were done in triplicate and the reproducibility of results was better than 3%.

RESULTS AND DISCUSSION

Figure 1 shows the adsorption–desorption N_2 isotherms for the selected samples TiO_2-A_{80}, AC and the binary TiO_2-A_{80}/AC material. Table 1 summarizes the BET surface area (S_{BET}) and surface pH (pH_{PZC}) of the samples. As reported elsewhere, commercial TiO_2 samples are non-porous materials (Matos *et al.* 2010a) in agreement with the low surface areas reported, and the surface pH detected varies from 6.4 for TiO_2-A_{80} up to 7.6 for TiO_2-A_0. It is important to point out that anatasase and rutile, $TiO_{2\text{-}A100}$ and TiO_2-A_0 respectively, showed lightly basic surface pH while the samples with mixtures of phases showed lightly acid surface pH. On the other hand, the AC showed a high surface area (880 m^2 g^{-1}) mainly composed of micropores in agreement with a type-I adsorption–desorption N_2 isotherm observed in Figure 1.

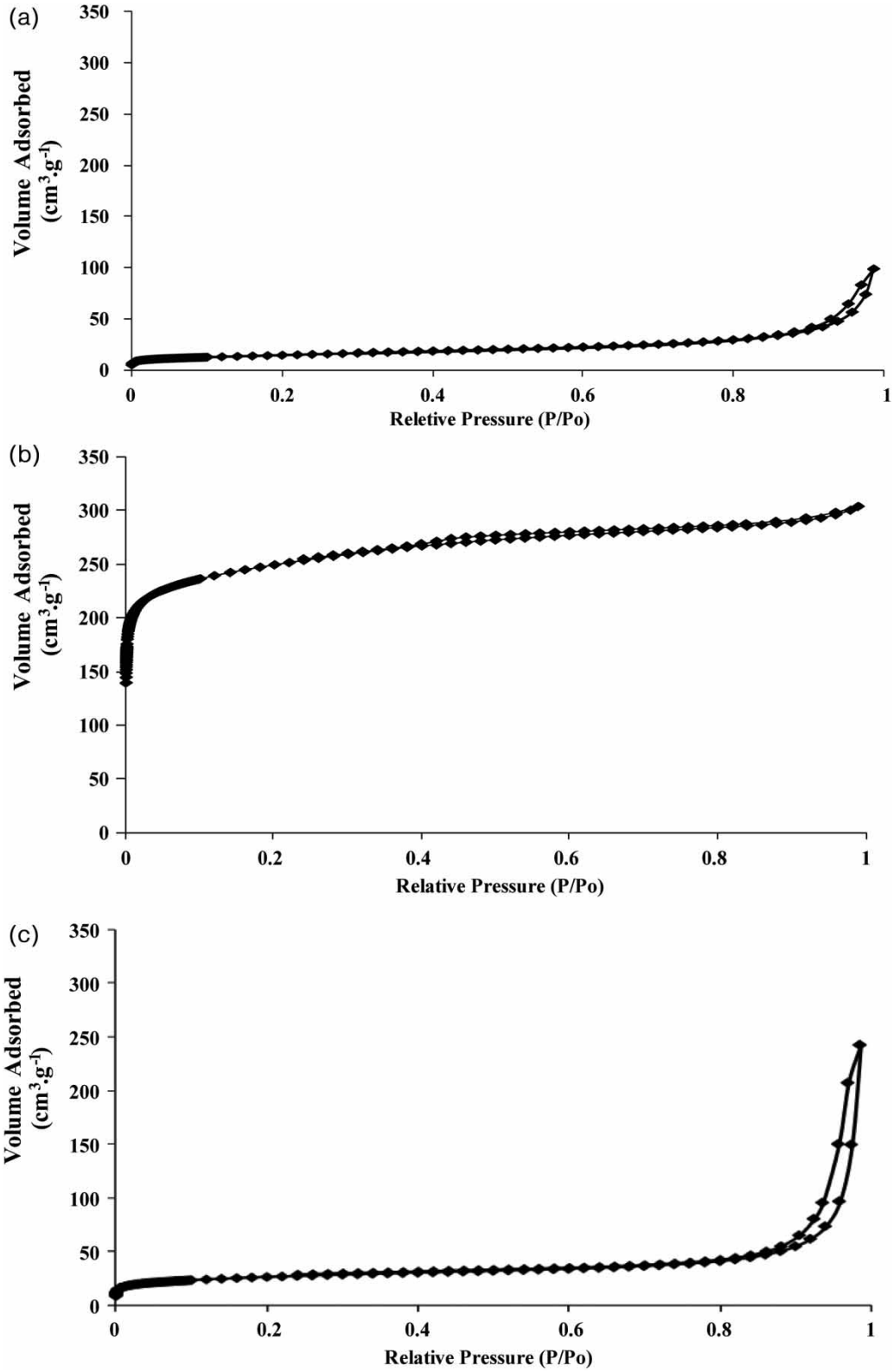

Figure 1 | Adsorption–desorption N_2 isotherms. (a) $TiO_2.A_{80}$. (b) AC. (c) $TiO_2.A_{80}$/AC.

Table 1 | Summary of BET surface area (S_{BET}) and surface pH (pH_{PZC})

Sample	S_{BET} ($m^2 g^{-1}$)	pH_{PZC}
TiO_2-A_{100}	25	7.3
TiO_2-A_{95}	11	6.8
TiO_2-A_{80}	54	6.4
TiO_2-A_0	13	7.6
AC	880	6.8
TiO_2-A_{100}/AC	104	6.8
TiO_2-A_{95}/AC	90	6.6
TiO_2-A_{80}/AC	129	6.3
TiO_2-A_0/AC	93	6.8

This AC showed an almost neutral surface pH indicating the presence of carbonyl groups on the surface. The binary materials showed representative surface areas of about 100 $m^2 g^{-1}$, a consequence of the contribution of AC and of a good dispersion of TiO_2 nanoparticles as suggested by the vertical hysteresis shown in the adsorption–desorption N_2 isotherms from Figure 1. The decrease in surface pH of all TiO_2 samples in presence of AC indicates a strong surface interaction between both solids.

Preliminary experiments of MB adsorption in the dark were performed to determine the weights of samples which should be used to obtain comparable amounts of MB adsorbed in order to correctly estimate the photocatalytic activity. These weights were 6.3 mg for AC and 62.5 mg for TiO_2 samples. In this sense, the kinetics of MB adsorption in the dark was assessed, and 60 min was obtained as the minimum time required to achieve the equilibrium of adsorption in the dark before start of the irradiation of samples. Table 2 shows a summary of the MB adsorbed in the dark after 60 min. It can be seen that AC and TiO_2/AC adsorbed much more MB than the TiO_2 samples. This is in agreement with the high surface area of AC and the representative surface area of the binary materials. However, it can be seen from the adsorption data in Table 2 that no additive effects were found for the MB adsorption in the dark in the binary materials. This phenomenon has been explained by our group (Matos *et al.* 2001; Cordero *et al.* 2007) as due to the formation of an intimate contact interface between both solids. It can be seen from Table 2 that, with the exception of TiO_2-A_0 and TiO_2-A_0/AC, the MB adsorbed in the dark after 60 min on the other three TiO_2 samples is between 0.8 and 1.0 μmol and on the other three TiO_2-AC samples is between 3.2 and 3.5 μmol. These values are very similar for each set of samples indicating that further kinetic estimation regarding the MB degradation to compare the photoactivity of each sample can be performed.

Figures 2 and 3 show the kinetics of MB photodegradation under UV and visible irradiation, respectively. It can be seen that the time required to total disappearance of MB is clearly shorter in presence of AC, indicating a beneficial influence of this support upon the photocatalytic activity of the different commercial titanium dioxides. This influence is detected even on the TiO_2-A_0 sample, which is the semiconductor with the lowest photoactivity as can be inferred from the high remaining MB concentration after 4 h irradiation.

The photocatalytic activity of the different phases of TiO_2 and the influence of AC can be estimated assuming a first-order reaction mechanism for the photodegradation of MB (Houas *et al.* 2007; Matos *et al.* 2011). Thus, the

Table 2 | Summary of kinetic results under UV and visible (Vis) irradiation. MB adsorption in the dark (MB_{ads}), first-order apparent rate-constants (k_{app}), regression linear factor (R^2), and photoactivity (ϕ_{rel}) of TiO_2/AC relative to TiO_2.

Sample	MB^a_{ads} (μmol)	k_{app}, UV (min^{-1}) × 10^{-3}	R^2, UV	ϕ^b_{rel} UV	k_{app}, Vis (min^{-1}) × 10^{-3}	R^2, Vis	ϕ^b_{rel} Vis
TiO_2-A_{100}	1.026	12.5	0.9965	[b]	12.6	0.9762	[b]
TiO_2-A_{95}	0.776	24.0	0.9929	[b]	15.3	0.9941	[b]
TiO_2-A_{80}	1.008	26.5	0.9736	[b]	19.4	0.9918	[b]
TiO_2-A_0	0.477	3.8	0.9426	[b]	1.0	0.9568	[b]
AC	2.763	5.3	0.9595	[b]	3.9	0.9198	[b]
TiO_2-A_{100}/AC	3.208	275.0	0.9185	22.0	208.9	0.9618	16.6
TiO_2-A_{95}/AC	3.472	216.6	0.9032	9.0	152.2	0.9061	9.9
TiO_2-A_{80}/AC	3.320	81.1	0.9420	3.1	111.4	0.9505	5.7
TiO_2-A_0/AC	2.584	5.6	0.9874	1.5	4.2	0.9566	4.2

[a]Estimated after 60 min adsorption in the dark.
[b]Relative photoactivity, ϕ_{rel}, was estimated for the binary materials from the ratio: $k_{app\text{-}TiO2/AC}/k_{app\text{-}TiO2}$.

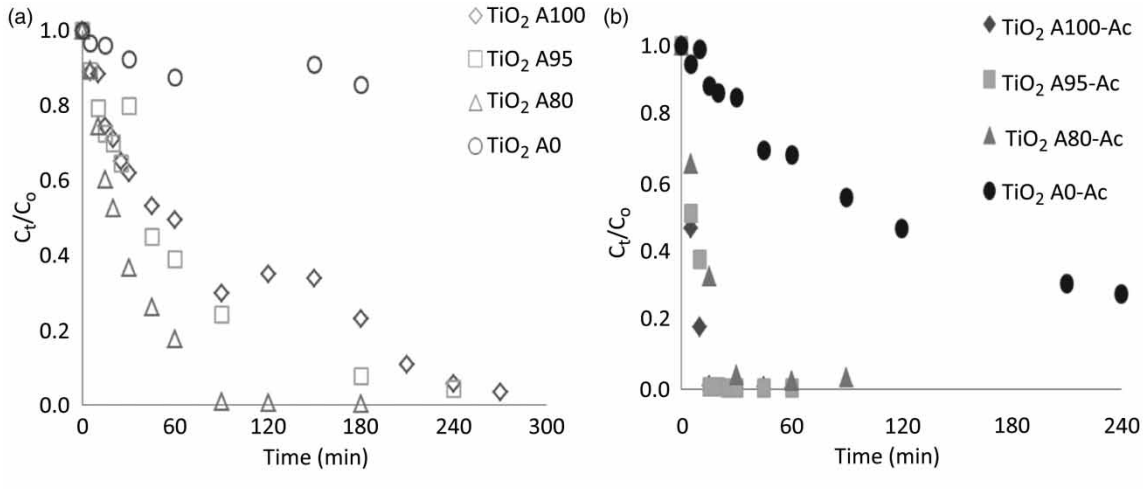

Figure 2 | Kinetics of MB disappearance on UV irradiation. (a) TiO_2 photocatalysts. (b) TiO_2/AC binary photocatalysts.

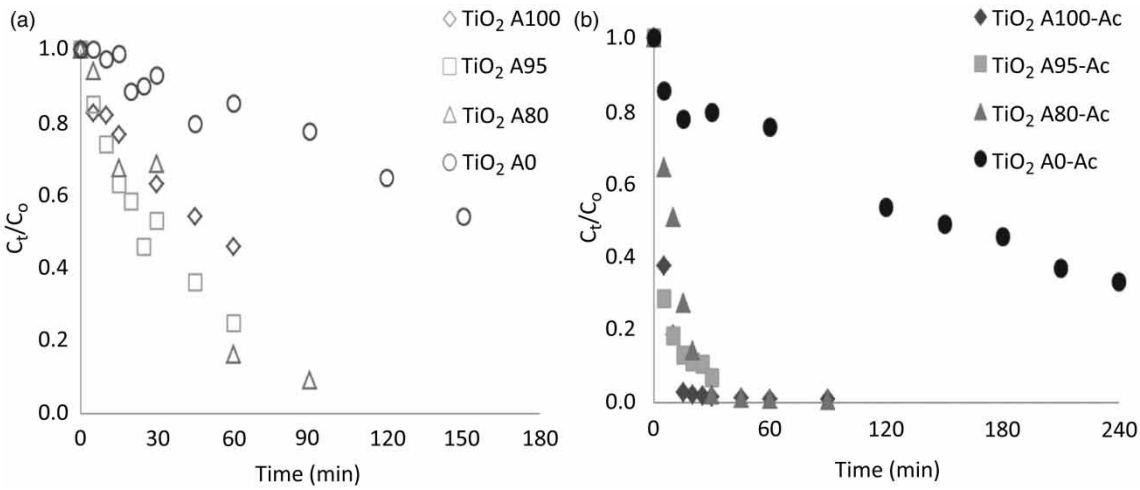

Figure 3 | Kinetics of MB disappearance under visible irradiation. (a) TiO_2 photocatalysts. (b) TiO_2/AC binary photocatalysts.

first-order apparent rate-constants (k_{app}) were obtained from the linear regression of the kinetic data from Figures 2 and 3. The k_{app} is the best kinetic parameter to verify the photoactivity of TiO_2/AC relative to TiO_2 (ϕ_{rel}). A summary of the kinetics parameters obtained for the photodegradation of MB on UV and visible irradiation is compiled in Table 2.

Interesting features can be seen from the first-order apparent rate-constants (k_{app}) and relative photoactivity (ϕ_{rel}) values in Table 2. As expected, k_{app} obtained on TiO_2 samples are higher under UV irradiation than under visible light. Also, it is important to remark that under both UV and visible irradiation the photocatalytic activity of pure anatase phase (TiO_2-A_{100}) is clearly much higher than that of rutile phase (TiO_2-A_0). This is in agreement with previous works (Yanagisawa & Ovenstone 1999) and can be attributed to the fact that anatase phase has one more oxygen vacancy than rutile phase in the TiO_2 crystalline framework (Bakardjieva *et al.* 2006).

It can be seen also from Table 2 that photocatalytic activity achieved a maximum value on UV- and visible-irradiated TiO_2-A_{80} photocatalysts. A combination of the oxygen vacancies in the TiO_2 framework with the representative surface area in this sample can be responsible of this maximum photoactivity. It is well known that up to now the commercial TiO_2 with about 80% anatase phase in the framework is commonly used as the standard semiconductor (P25 from Evonik) in heterogeneous photocatalysis.

By contrast, it is important to point out that in presence of AC the TiO_2/AC binary materials remarkably change the photocatalytic trends in comparison with neat TiO_2. It can be seen from k_{app} and ϕ_{rel} in Table 2 that under both types of irradiation, the TiO_2/AC followed an exponential increase in the photocatalytic activity as a function of anatase proportion in the TiO_2 framework. This trend can be seen in Figure 4 for the two types of irradiation. It can be seen that the pre-exponential factor is higher in the case of UV irradiation (5.3 against 4.3 min^{-1}) while the argument of the exponential function is practically similar in both types of irradiation, suggesting that the TiO_2 crystalline framework is related to the pre-exponential factor, which is related to the kinetic parameters. By contrast, the specific characteristics of the AC seem to be related to the exponential argument, because it is the constant component of the binary materials of the present study.

In other words, the higher the anatase proportion the higher the photocatalytic activity of the binary material and this increase is clearly exponential up to 22 and about 17 times higher under UV and visible irradiation, respectively. To the best of our knowledge, this exponential influence of AC upon the photocatalytic activity of TiO_2 as a function of the anatase proportion in the crystalline framework is reported for the first time in this work. This behavior is still under evaluation and studies are being performed by UV-Vis diffuse reflectance (UV-Vis/DR) and RAMAN spectroscopy to verify changes in the optical band of the semiconductor as a function of the anatasase:rutile ratio. The present results suggest a very effective contact interface created between both solids (Matos *et al.* 1999, 2001), which is clearly enhanced by the highest oxygen vacancies in the anatase TiO_2 sample. We have already reported in a previous work (Matos *et al.* 2010a) with X-ray photoelectronic spectroscopy and X-ray absorption near edge structure spectroscopy (XANES) that oxygenated functional groups in the surface of AC can be coordinated to the TiO_2. This work showed that during the reaction, an important interfacial interaction occurred between TiO_2 and AC. For example, Ti K-edge XANES spectra for TiO_2 and TiO_2-AC binary materials showed a reduction in the oxygen vacancies of TiO_2 as a consequence of the interaction with the oxygenated surface groups on AC. In addition, functional surface groups on AC are able to promote the donor of photoexcited electrons from π to π^* orbitals in these functional groups, mainly pyrones and quinones, and thus become a photo-assistance agent (Matos *et al.* 2010b) enhancing the TiO_2 photoactivity even under visible light. This fact has been recently confirmed by S-doped (Bandosz *et al.* 2012) and N-doped (Matos *et al.* 2013) AC.

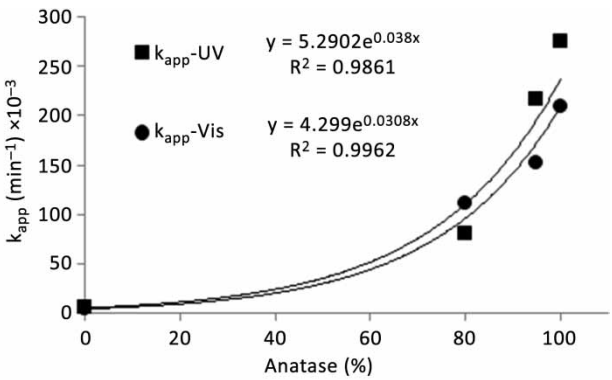

Figure 4 | Influence of the anatase crystalline proportion upon the first-order apparent rate-constants for the MB photodegradation under UV- and visible irradiation of TiO_2-AC binary photocatalysts.

CONCLUSIONS

The photocatalytic activity of different crystalline TiO_2 phases and the influence of AC was verified in the photocatalytic degradation of MB under UV and solar irradiation. Results showed a maximum photoactivity for the crystalline phase ratio of anatasase:rutile equal to 80:20 both under UV and solar irradiation, while the TiO_2/AC binary materials followed an exponential increase in the photocatalytic activity, as a function of anatase proportion in the TiO_2 framework, up to 22 and about 17 times higher under UV and visible irradiation, respectively. The present results suggest that AC interacts more efficiently with anatasase phase than rutile phase.

REFERENCES

Andreozzi, R., Caprio, V., Insola, A. & Marotta, R. 1999 Advanced oxidation processes (AOP) for water purification and recovery. *Catalysis Today* **53** (1), 51–55.

Araña, J., Rodriguez, J. M., Tello, E., Garriga, C., Gonzalez, O., Herrera-Melián, J. A., Pérez-Peña, J., Colón, G. & Navío, J. A. 2003 TiO_2 activation by using activated carbon as a support. Part II. Photoreactivity and FTIR study. *Applied Catalysis B: Environmental* **44** (2), 153–160.

Bacsa, R. R. & Kiwi, J. 1998 Effect of rutile phase on the photocatalytic properties of nanocrystalline titania during the degradation of p-coumaric acid. *Applied Catalysis B: Environmental* **16** (1), 19–29.

Bakardjieva, S., Stengl, V., Szatmary, L., Subrt, J., Lukac, J., Murafa, N., Niznansky, D., Cizek, K., Jirkovskyc, J. & Petrovad, N.

2006 Transformation of brookite-type TiO_2 nanocrystals to rutile: correlation between microstructure and photoactivity. *Journal of Materials Chemistry* **16** (18), 1709–1716.

Bandosz, T. J., Matos, J., Seredych, M., Islam, M. S. Z. & Alfano, R. 2012 Photoactivity of S-doped nanoporous activated carbons: a new perspective for harvesting solar energy on carbon-based semiconductors. *Applied Catalysis A: General* **445–446**, 159–165.

Cordero, T., Duchamp, C., Chovelon, J.-M., Ferronato, C. & Matos, J. 2007 Influence of L-type activated carbons on photocatalytic activity of TiO_2 in 4-chlorophenol photodegradation. *Journal of Photochemistry and Photobiology A: Chemistry* **191** (2–3), 122–131.

Ha, P. S., Youn, H. J., Jung, H. S., Hong, K. S., Park, Y. H. & Ko, K. H. 2000 Anatase–rutile transition of precipitated titanium oxide with alcohol rinsing. *Journal of Colloid and Interface Science* **223** (1), 16–20.

Herrmann, J.-M., Matos, J., Disdier, J., Guillard, C., Laine, J., Malato, S. & Blanco, J. 1999 Solar photocatalytic degradation of 4-chlorophenol using synergistic effect between titania and activated carbon in aqueous suspension. *Catalysis Today* **54** (2–3), 255–265.

Hotsenpiller, P. A. M., Bolt, J. D., Farneth, W. E., Lowekamp, J. B. & Rohrer, G. S. 1998 Orientation dependence of photochemical reactions on TiO_2 surfaces. *Journal of Physical Chemistry B* **102** (17), 3216–3226.

Houas, A., Lachheb, H., Ksibi, M., Elaloui, E., Guillard, C. & Herrmann, J.-M. 2007 Photocatalytic degradation pathway of methylene blue in water. *Applied Catalysis B: Environmental* **31** (2), 145–157.

Lopez-Ramon, M. V., Stoeckli, F., Moreno-Castilla, C. & Carrasco-Marin, F. 1999 On the characterization of acidic and basic surface sites on carbons by various techniques. *Carbon* **37** (8), 1215–1221.

Matos, J., Laine, J. & Herrmann, J.-M. 1998 Synergy effect in the photocatalytic degradation of phenol on a suspended mixture of titania and activated carbon. *Applied Catalysis B: Environmental* **18** (3–4), 281–291.

Matos, J., Laine, J. & Herrmann, J.-M. 1999 Association of activated carbons of different origins with titania in the photocatalytic purification of water: use of solar energy. *Carbon* **37** (11), 1870–1872.

Matos, J., Laine, J. & Herrmann, J.-M. 2001 Effect of the type of activated carbons on the photocatalytic degradation of aqueous organic pollutants by UV-irradiated titania. *Journal of Catalysis* **200** (1), 10–20.

Matos, J., Laine, J., Herrmann, J.-M., Uzcategui, D. & Brito, J. L. 2007 Influence of activated carbon upon titania on aqueous photocatalytic consecutive runs of phenol photomineralization. *Applied Catalysis B: Environmental* **70** (1–4), 461–469.

Matos, J., García, A. & Poon, P. S. 2010a Environmental green chemistry applications of nanoporous carbons. *Journal of Materials Science* **45**, 4934–4944.

Matos, J., García-López, E., Palmisano, L., García, A. & Marci, G. 2010b Influence of activated carbon in TiO_2 and ZnO mediated photo-assisted degradation of 2-propanol in gas–solid regime. *Applied Catalysis B: Environment* **99** (1–2), 170–180.

Matos, J., Rosales, M., García, A., Nieto-Delgado, C. & Rangel-Mendez, J. R. 2011 Hybrid photoactive materials from municipal sewage sludge for the photocatalytic degradation of methylene blue. *Green Chemistry* **13** (12), 3431–3439.

Matos, J., Hofman, M. & Pietrzak, R. 2013 Synergy effect in the photocatalytic degradation of methylene blue on a suspended mixture of TiO_2 and N-containing carbons. *Carbon* **54**, 460–471.

Ren, W., Ai, Z., Jia, F., Zhang, L., Fan, X. & Zou, Z. 2007 Low temperature preparation and visible light photocatalytic activity of mesoporous carbon-doped crystalline TiO_2. *Applied Catalysis B: Environmental* **69** (3–4), 138–144.

Torimoto, T., Okawa, Y., Takeda, N. & Yoneyama, H. 1997 Effect of activated carbon content in TiO_2-loaded activated carbon on photodegradation behaviours of dichloromethane. *Journal of Photochemistry and Photobiology A: Chemistry* **103** (1–2), 153–157.

Tryba, B., Morawski, A. W., Inagaki, M. & Toyoda, M. 2006 The kinetics of phenol decomposition under UV irradiation with and without H_2O_2 on TiO_2, Fe-TiO_2 and Fe-C-TiO_2 photocatalysts. *Applied Catalysis B: Environmental* **63** (3–4), 215–221.

Yanagisawa, K. & Ovenstone, J. 1999 Crystallization of anatase from amorphous titania using the hydrothermal technique: Effects of starting material and temperature. *Journal of Physical Chemistry B* **103** (37), 7781–7787.

Wang, W., Gomez Silva, C. & Faria, J. L. 2007 Photocatalytic degradation of chromotrope 2R using nanocrystalline TiO_2/activated-carbon composite catalysts. *Applied Catalysis B: Environmental* **70** (1–4), 470–478.

First received 19 November 2013; accepted in revised form 24 February 2014. Available online 10 March 2014